Microscopic Mechanical Properties and Injection Molding-Induced Morphology on Polypropylene Rubber Blend

Yutaka Kobayashi,[1,2] Makoto Ando,[3] Toshitaka Kanai[2,3]

[1]*Research and Development Division, Prime Polymer Company Limited, 580-30 Nagaura, Sodegaura-City, Chiba 299-0265, Japan*
[3]*Division of Material Sciences, Graduate School of Natural Science & Technology, Kanazawa University, Kakuma-Machi, Kanazawa-City, Ishikawa 920-1192, Japan*
[2]*Research and Development Laboratory, Idemitsu Kosan Company Limited, Anasaki-Kaigan, Ichihara-City, Chiba 299-0193, Japan*

Received 23 May 2009; accepted 28 November 2009
DOI 10.1002/app.31878
Published online 20 January 2010 in Wiley InterScience (www.interscience.wiley.com).

ABSTRACT: A microdeformation of a simple polymer blend of polypropylene (PP) and ethylene butene rubber (EBR) was investigated in this study. Injection molding-induced morphology close to the surface was analyzed by transmission electron microscope, polarizing optical microscope, and Fourier transform IR spectroscopy. Breakup and coalescence of EBR particles scarcely occurred during the injection process. The EBR particles near the surface were observed as continuous fibers and were gradually changing to the ellipsoidal shape in the depth direction. The morphology in an injection molded specimen was related to depth profiles of mechanical factors, which were microhardness and shear stress measured by a Vickers and a Knoop microindenter and "Surface and Interface Cutting Analysis System," respectively. Crystal structure of PP matrix affected to the microdeformation more strongly than that of EBR phase. The large oriented EBR domains disconnected continuity of the PP matrix and acted as a weak layer in the specimens. Finally, cohesive fracture occurred in the peel test of painted PP/EBR was discussed from a microdeformation point of view. © 2010 Wiley Periodicals, Inc. J Appl Polym Sci 116: 2590–2600, 2010

Key words: microdeformation; injection molding; morphology; poly(propylene)

INTRODUCTION

Polypropylene (PP) is widely used in the automotive industry because it is lightweight, inexpensive, recyclable, and easily processed by injection molding. The properties of PP are modified by adding fillers, elastomers, and many kinds of additives to satisfy the required specifications for automotive parts, such as bumper fascia, door panels, and dashboards. Recently, the surface properties of injection molded PP have become more important for automotive parts because of environmental reasons. Better paintability of PP is required for the painting system from which volatile organic solvents are eliminated. In some cases painting itself is disused, therefore, better scratch resistance is an essential property for automotive parts. The modified PP is often called thermoplastic polyolefins (TPO). Painting for PP is more difficult than that of steel, because chemical affinity between PP and paints is very poor. Therefore, a chlorinated polyolefin (CPO) based adhesion promoter was used as an intermediate binder, which penetrates into the substrate. The depth of penetration was affected by a content of elastomers in the substrates and organic solvent in the paint.[1] Adhesiveness between substrates and paints was generally evaluated by a 180 degrees peel test, in which the peel strength was increased with adding an elastomer.[2] An adherence improved by the presence of the elastomer domain was explained by energy dissipation occurred during the rubber deformation.[3] We are interested in the relationship between the peel strength and elastomer morphology in an injection molded plaque of TPO, because automotive parts are mainly produced by injection molding. In the previous studies, the position of debonding was not located at an interface between a coated film and a substrate but the layer inner the surface.[4] The relationship between the peel strength and a formulation of a commercial TPO were too complex.[5] Therefore, the purpose of our work is to clarify a microdeformation on an injection molded polymer blend of PP and ethylene butene rubber (EBR), which is precisely characterized morphology of elastomer near the surface.

A lot of previous studies deal with morphology of TPO.[6–9] There are two types of the PP blends for commercial TPO. In the case of a reactor blend,

Correspondence to: Y. Kobayashi (y.kobayashi-@nifty.com).

ethylene propylene rubber (EPR) is polymerized into PP by a series of reactors. For extruder blend, EBR and/or ethylene octene rubber (EOR) are mainly mixed into PP. Injection molding-induced morphology of PP/EPR blends was very complex. Shapes of EPR domains in PP matrix were varied from surface to core in a molded specimen. Spherical droplets were located in the core region and oriented droplets were near the surface to the flow direction. During the injection process, EPR particles were subject to deformation, breakup, and coalescence.[6] Same morphological changes were also observed with a blends of PP and EOR.[7] From the comparison of the EPR microstructure between a titanium (Ti) and a vanadium (V) based catalytic system, crystallinity and lamellar thickness of PP in the blends were reduced by adding 40 wt % of Ti-EPR.[8,9] EPR with lower ethylene content was miscible in PP.[10] These varieties of morphology affect the peel strength on a painted injection-molded plaque. Our question is what factor is controlling the position where cohesive delamination of the substrate occurs in the peel test. The weakest point from surface to core in an injection-molded specimen was found out with using an instrumented microindentation and a "Surface and Interface Cutting Analysis System (SAICAS)."

Microhardness was used for the evaluation of a microscopic deformation of polymer blends.[11–14] Polymer blends consisting of soft and hard components frequently showed drastic deviations from the additivity law for calculation of overall microhardness. Although many types of morphology was observed in the blends, the microhardness was estimated by a volume fraction and a glass transition temperature of each component.[11] The deviation was also measured for reactor blends of PP and EPR, which had spherical EPR domains in PP matrix. The overall microhardness was affected by reducing partial microhardness of PP crystals, because EPR increased interfacial energy on PP crystal.[12] From the precise polymerization of styrene–butadiene block copolymer, unique matrix – domain structures were made in specimens for a microhardness measurement. The microhardess of the samples containing the same amount of styrene was changed by the morphology, such as cylinders and alternatively stacking lamellae.[13] In the case of lamellar morphology, the microhardness was proportional to the thickness of the polystyrene lamellae.[14] Although the deformation on the surface can be measured by the indentation method, the method is unsuited for detecting continuous changes of the deformation in the depth direction. On the other hand, SAICAS is suitable for continuous measurements of shear stresses, for example, the characterization of interfacial adhesion in multilayered paint films.[15]

In this article, we focus on injection molding-induced morphology, which affect the position occurred fracture or large deformation during the peel test. Matrix-domain structure of a PP/EBR blend was analyzed precisely, and then the structure was compared to a microscopic deformation from surface to core in an injection-molded specimen. The transmission electron microscope (TEM) was used for evaluating rubber particles and their distributions. Crystal structure from skin to core was analyzed by birefringence with Polarizing optical microscope (POM). A deformation behavior of PP/EBR with highly oriented morphology was investigated by an instrumented microindenter with a Vickers pyramid diamond and a Knoop rhombic-based pyramid diamond. Debonding mechanism of the painted TPO was estimated from a shear stress distribution in the depth direction of injection molded specimens by SAICAS.

EXPERIMENTAL

Material

A polymer blend of PP/EBR was used in this study. Characteristics of PP were Ziegler–Natta isotactic homopolymer (MFR 13 g/10 min for 2.16 kg at 230°C, pentad ratio 97%), molecular weight (Mw 306 kg/mol, Mw/Mn 8.3), and nucleating agent was added. EBR was A4050S, a commercial product from Mitsui Chemical. The PP/EBR (77.2 wt %/22.8 wt %) blend was mixed by a twin-screw extruder, TEM-30 (Toshiba), with a barrel temperature of 200°C.

Preparation of specimen

An injection molded plaque and a compression molded plaque was prepared for comparing morphology of elastomer in the blend of PP/EBR. As shown Table I, the molten resin in injection molding is solidified in the cold cavity during flowing, so oriented morphology is generally observed. On the other hand, unoriented morphology is formed by compression molding, because molten resin is shaped at high temperature.

Injection molding was carried out by an injection-molding machine, IS100F-III (Toshiba), using a tool of a rectangular plaque ($^{w}70 \times {}^{l}270 \times {}^{t}3$ mm). Pellets of PP/EBR were molten during plasticating process at barrel temperature 200°C. The molten resin was injected for 3 s filling time into the cavity of the tool, which is at 40°C of mold temperature. And then, holding pressure was applied for 8 s in order to avoid a deformation caused by volumetric shrink during cooling. Finally, the molded plaque was cooled for curing time 20 s after shutting off the holding pressure.

TABLE I
Thermal and Flow History of PP/EBR in Injection and Compression Molding

	Melting	Shaping	Cooling
Injection molding			
Temperature	200°C	200 –> 20°C	20°C
Process time	20 s	3 s	20 s
Machine motion	Rotating screw	Injection	Static
Compression molding			
Temperature	200°C	200°C	200°C –> 20 °C
Process time	5 min.	2 min	5 min
Machine motion	Static	Compression	Static

Compression molded was manually carried out by a hot pressing machine using a steel spacer ($^{w}150 \times {}^{l}150 \times {}^{t}3$ mm). Pellets of 61 g were placed between aluminum plates with the spacer and molten at 200°C for 5 min, and then compressed at 200°C for 2 min. Finally, shaped molten polymer with the plates was moved into a cold pressing machine and quenched at 20°C for 5 min.

Microhardness measurements

Microhardness was measured using an Elionix ENT-1100a tester at room temperature. A Vickers and a Knoop indenter tips were used for the experiment and microhardness data using these indenter tips were given by H_V and H_K, respectively. The hardness values based on H_V and H_K are not directly comparable. The Vickers hardness is calculated by the contact area, whereas the Knoop hardness is based on the projected area. Studied positions for injection molded plaques were located close to the center of the part (Fig. 1). Measurements were performed on the surface of molded plaques and the cross-cut surface parallel to the flow direction (edge view). For compression molded specimens, the center position was studied. The cross-cut surface was polished by a Buehler Ecomet 3000 apparatus with 0.05 μm alumina paste. To evaluate anisotropy of the specimens, the long diagonal of the knoop indenter was applied to the flow direction (FD) and the perpendicular direction, more specifically, the transverse direction (TD) on the molded surface and the normal direction (ND) on the cross-cut surface.

Shear stress measurement

To profile a distribution of shear stress along the depth direction of injection molded specimens, SAICAS DN-20S (Daipla Wintec) was used in this experiment. A diamond tip with 1 mm width cut at the 10 μm depth with the 20 μm/s horizontal speed. The principle of the measurement was based on the cutting theory.[16] A shear plane angle was derived from the Merchant equation with a friction angle and a rake angle. Cutting depth was measured by a confocal laser scanning microscope (LSM), Optelics H1200 (Lasertec).

Motion of SAICAS for paintability resembles the Hesiometer which shaves coats from substrates [Fig. 2(a)].[17] Although the adhesion strength between coats and substrates was measured using SAICAS,[15] we applied it for profiling of shear stresses in the depth direction [Fig. 2(b)]. Injection molded specimens, which had the skin-core structure, were bonded with CPO (thickness 2.1 μm). This experiment clarified a weak point which was related to the

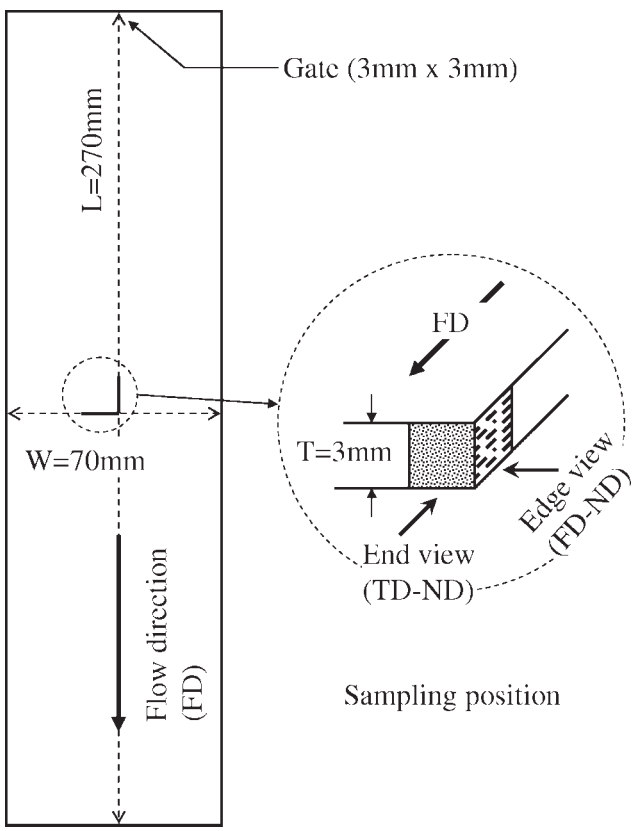

Figure 1 A schematic diagram of an injection molded plaque and specimens cut at the central position.

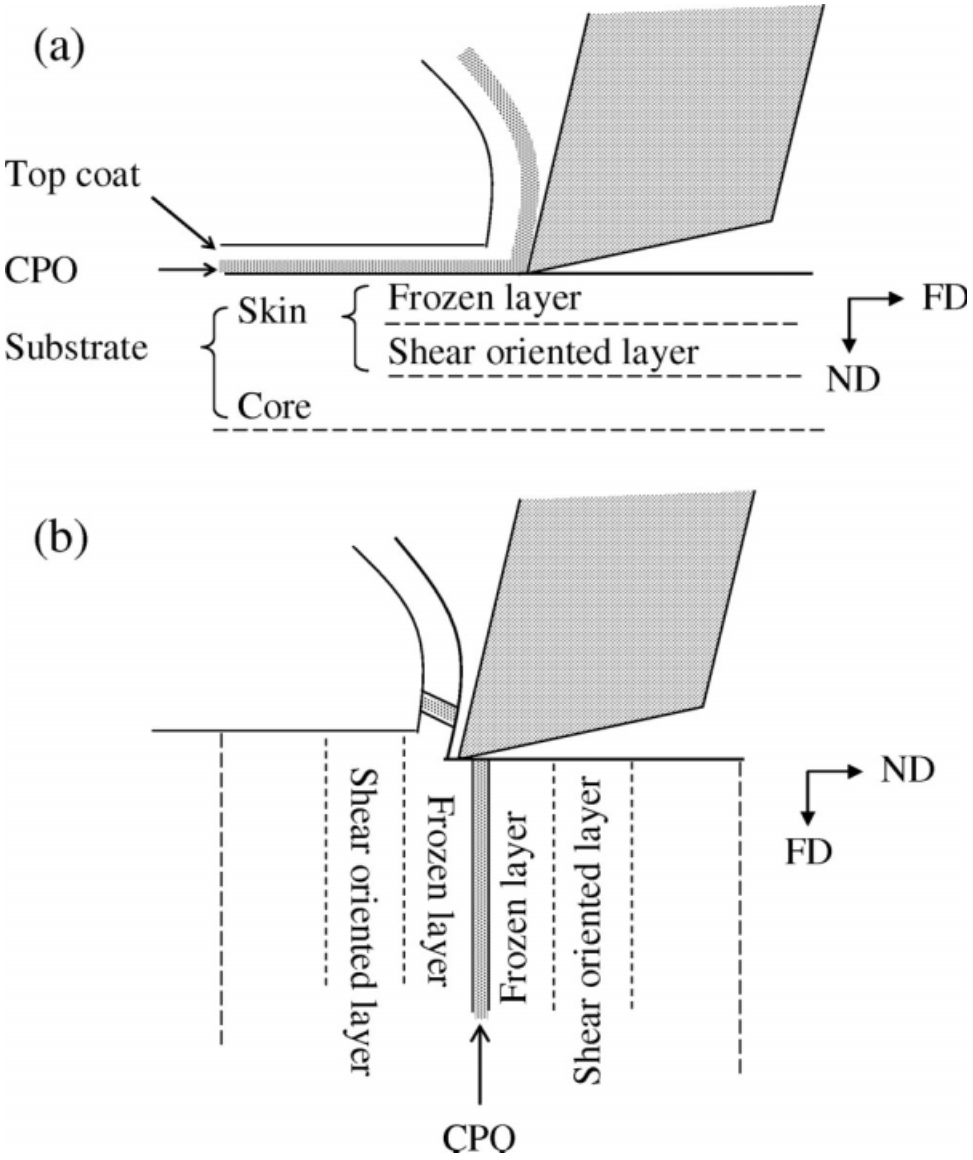

Figure 2 Schematic diagrams of a cutting direction for SAICAS; (a) a general method and (b) a depth profiling method.

injection molding-induced morphology. Specimens were pretreated in the same way as the microhardness measurement. Cross-cut surfaces of parallel and perpendicular to the flow direction were compared. In addition, adhesion of the molded specimens were carried out with CPO, Superchlon 822 (Nippon paper chemicals), at 80°C for 30 min.

Morphological characterization

The specimens were characterized by POM, TEM, FTIR, and LSM. The POM observation was carried out using Olympus BH-2 with a Berek compensator at room temperature. Studied positions were located in the middle of the molded plates (Fig. 1). A crystal structure of the microtomed section was viewed parallel to the flow direction (edge view).

Morphology of EBR in the PP matrix was observed by TEM, JEM-1010 (JEOL). Specimens were stained with ruthenium tetroxide (RuO_4) vapor at 25°C for 15 h. EBR domains dispersed in PP matrix were stained mainly. Little change in PP matrix occurred so the contrast between the matrix and domains became sharp. Ultrathin sections were microtomed from the stained specimens by Leica EM UC6. The observations were carried out parallel and perpendicular to the flow direction at the center of the plaque (Fig. 2). Each direction was distinguished by "Edge view" and "End view". Stained dark phases were rubber portions. Quantification of the dispersed phase was carried out by the image analysis with software, ImageJ (National Institute of Mental Health).[18] Particle size was determined by a histogram of the particle area. Shape of the particle

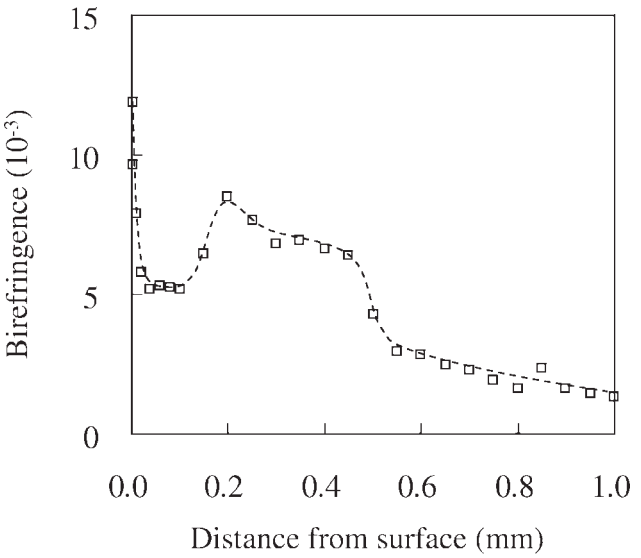

Figure 3 Changes in birefringence from surface to core of the injection molded specimen of PP/EBR.

was evaluated by circularity. The definition of the circularity is 4π (area)/(perimeter)^2, so that the circularity equals 1 for circles and close to 0 for fibrous stretched shapes.

The FTIR experiment was carried out with a Nicolet 8700 and Continuum microscope at room temperature. The equipment was operated in transmission mode with 100 scans per sampling at a resolution of 4 cm^{-1} in the wavenumber range between 4500 and 650 cm^{-1}. Observed positions in the specimen were the same as those for the microharness experiment. The microtomed cross-cut section of the specimen, 40 μm thickness, was measured with an aperture size of 50 μm × 150 μm in the normal direction. All spectra were collected for background spectra to remove the atmospheric effects such as carbon dioxide and the moisture in the air.

Surface roughness and thicknesses of coated layers were analyzed by LSM. Microphotographs were taken with a green lay (wavelength 546 nm). The

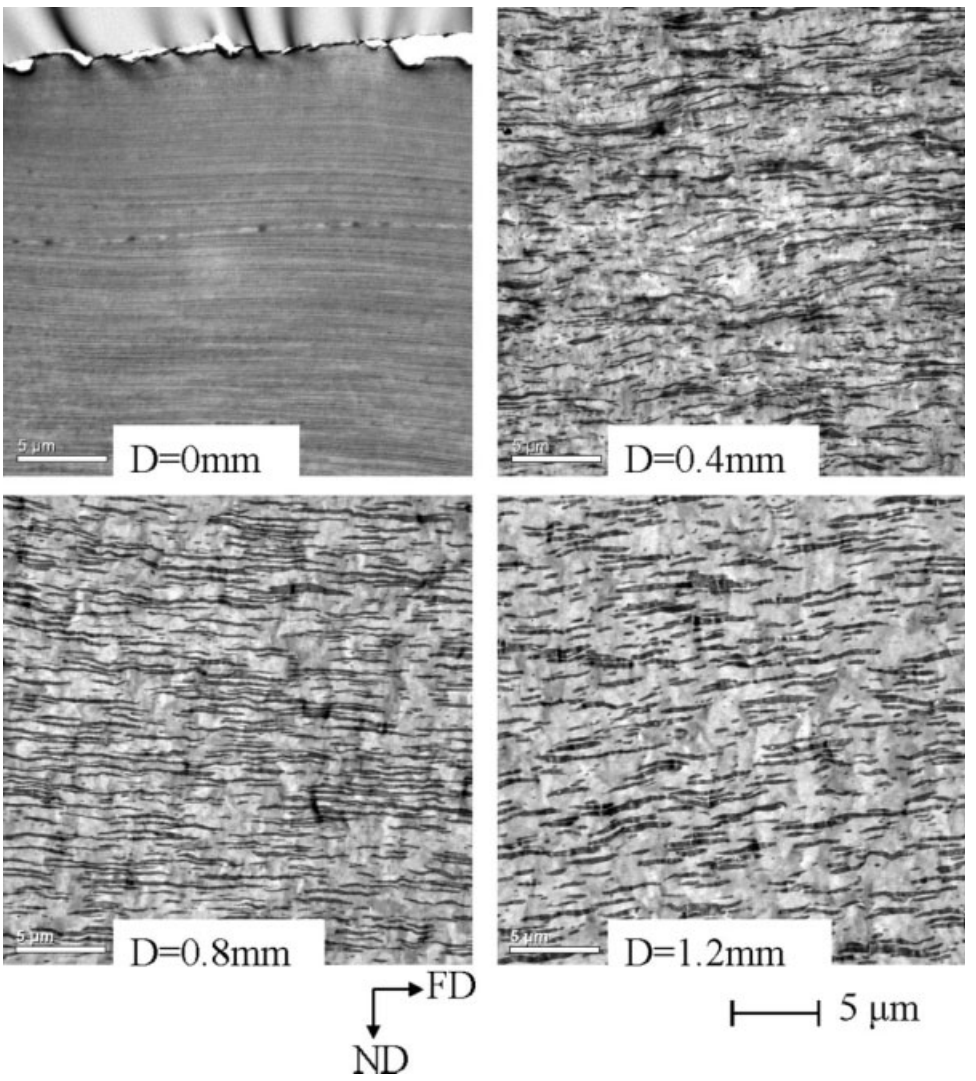

Figure 4 TEM photographs of PP/EBR from surface to core in the injection molded plaque observed cross-cut thin section parallel to the flow direction (FD-ND).

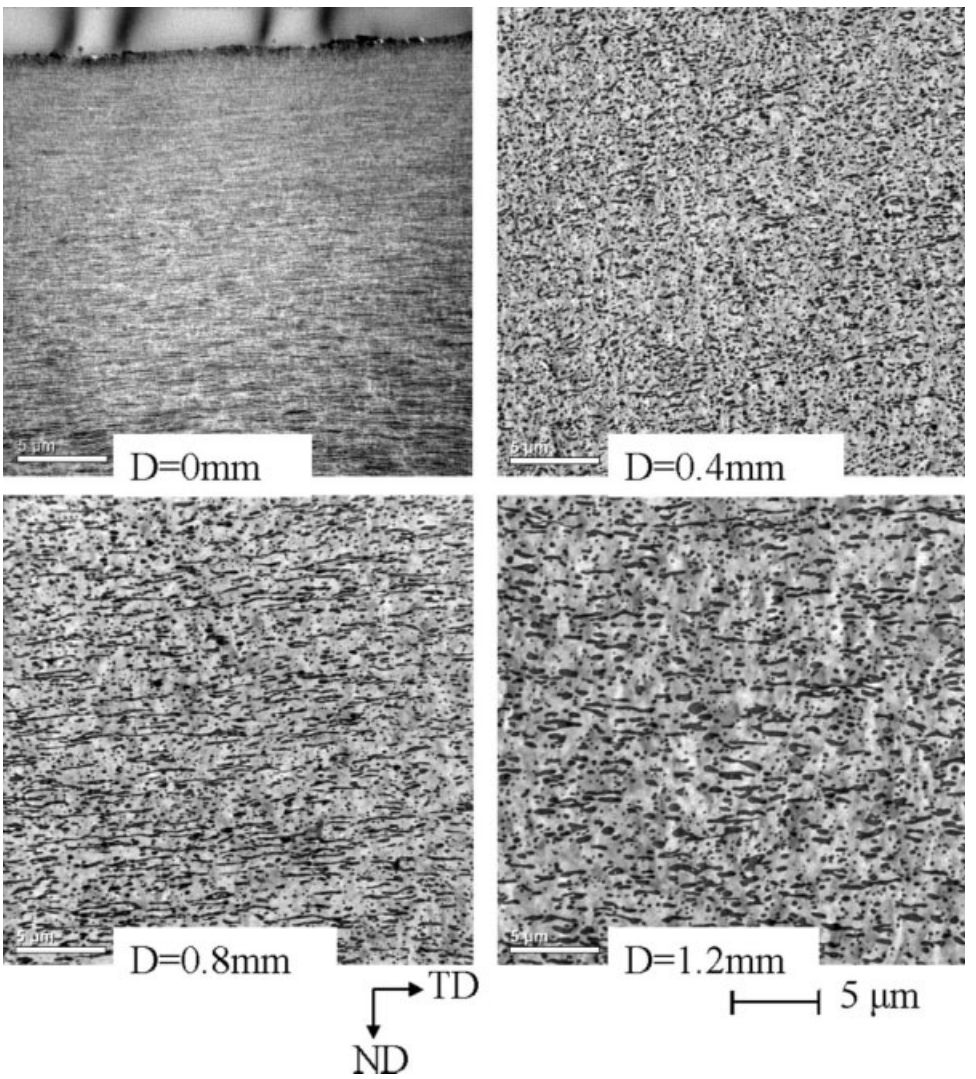

Figure 5 TEM photographs of PP/EBR from surface to core in the injection molded plaque observed cross-cut thin section perpendicular to the flow direction (TD-ND).

measured positions were indicated in each case. Observation of the peeled surface was carried out with scanning electron microscopy (SEM), JSM-5600LV (JEOL), instead of LSM. The samples were prepared by sputtering of gold using Auto Fine Coater JFC-1600 (JEOL).

Peel strength

Injection-molded plaques were painted as follows: degreasing by aqueous soap and rinsing with distillated water, spraying the CPO based adhesion promoter; after 10 min, spraying urethane top coat (so-called wet on wet system) and baking at 80°C for 45 min. After 48 hrs, painted specimens were measured for the 180 degrees peel strength (ISO 8510-2). Peel conditions are as follows: peel speed 50 mm/min, width 10 mm, and at room temperature.

RESULTS AND DISCUSSION

Rubber morphology along the depth direction

Elastomer morphology in an injection-molded specimen is related to adhesion strength between TPO substrates and paints.[2–5] At first, the morphology near the surface in a simple polymer blend of PP and EBR was precisely characterized using POM and TEM. Observed thin sections were cut parallel and perpendicular to the flow direction at the middle of the injection molded plaque (Fig. 1). Molecular and crystal orientations in the specimen were observed at the edge thin film (0.03 mm) of PP/EBR by POM. As shown in Figure 3, the birefringence near the surface decreased sharply and reached the local minimum at the 0.1 mm depth. The frozen layer was formed by rapid freezing of the highly stretched polymer. Then the birefringence increased along the depth direction due to the shear

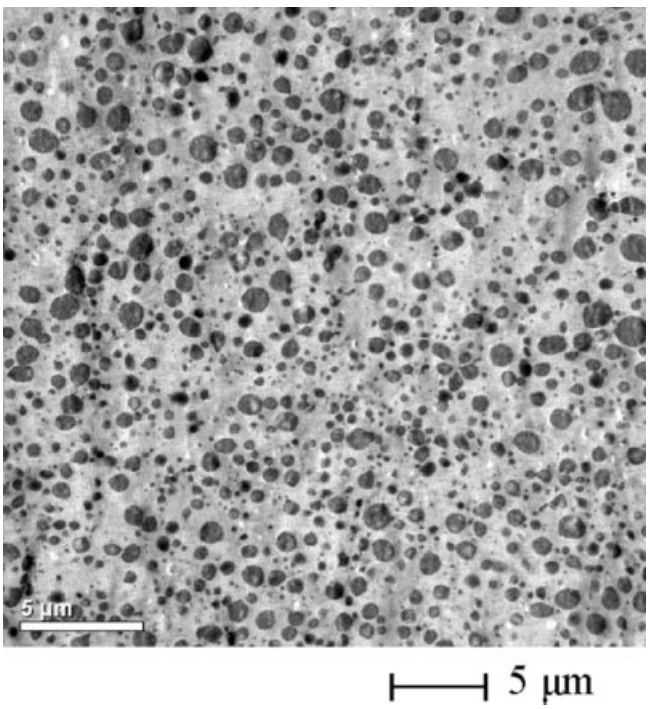

Figure 6 A TEM photograph of PP/EBR from surface to core in the compression molded plaque observed cross-cut thin section.

orientation in the filling process. The thickness of the shear oriented layer was 0.4 mm. This typical skin-core microstructure occurs when molecular chains in the skin layer is highly oriented to the flow direction because of the high strain-rates and rapid cooling imposed during processing.[19]

The morphology of EBR phase in the injection molded specimens was observed by TEM. As shown in Figure 4, EBR domain was fibrous through the edge view. On the other hand, dot-like dispersion was observed through the end view (Fig. 5). That means particles deform in the shape of a rod during injection molding. The deformation of EBR is gradually reducing from surface to core. Although high birefringence is observed at the surface and a shear oriented layer for PP, orientation of EBR does not show the local maximum along the depth direction. For a compression molded specimen spherical morphology was observed (Fig. 6). Quantification of the morphological difference in the molding methods was carried out by the image analysis. A domain size and circularity was used as parameters in this study. The circularity equals 1 for circles and close to 0 for fibrous stretched shapes. As shown in Figure 7, the histograms of the particle area are almost same in the depth position of the injection molded specimen and compression molded one, whereas the histograms of the circularity show opposite patterns in the molding methods. Thus, visual impression of the TEM photographs was characterized numerically. From the results of the image analysis, breakup, and coalescence of EBR particles scarcely occur during the injection process except the changes at the surface region. Since the EBR particles near the surface are strongly stretched and observed as continuous fibers in the edge view, whole size of the fibrous EBR could not be distinguished in TEM study. Therefore, the area and circularity near the surface were not analyzed.

Although the orientation of EBR gradually decreases from surface to core, the birefringence indicates local minimum and maximum values. Molecular and crystal orientation of PP was different from the orientation of EBR particles. Therefore, we investigated next which factor affects strongly to the microdeformation in the injection molded specimen.

Influence of morphology on microhardness

The depth profiles of the microhardness with a Vickers tip (H_V) were measured on the cross-cut surface (MD-ND) of the injection and compression molded specimens (Fig. 8). For the compression molded

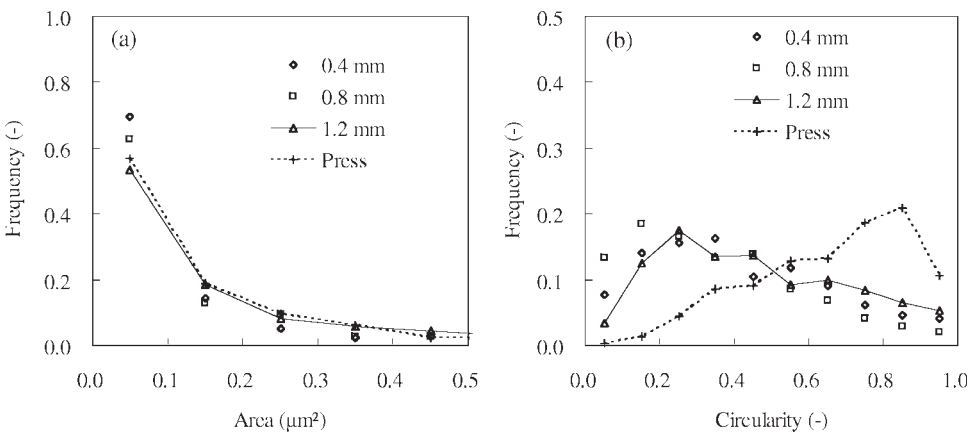

Figure 7 Distribution of EBR particles in the depth direction; (a) area and (b) circularity. The data were image-analyzed from Figure 4, 5, and 6.

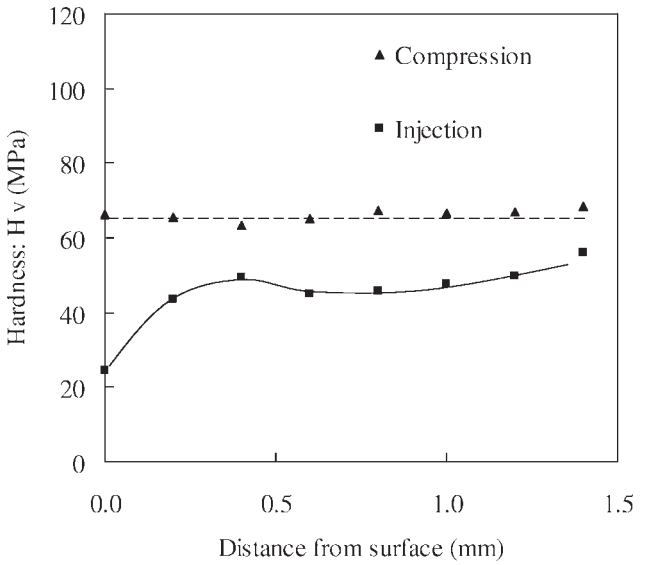

Figure 8 Microhardness (H_V) near the surface in the injection molded plaque. Measurement conditions: indentation load 10 m*N*, room temperature.

specimen, H_V stayed constant to the depth direction. In the case of the injection molding, H_V indicated minimum at the surface and local maximum at the 0.4 mm depth, which were corresponding to the shear oriented layer in Figure 3. The indentation depth was varied from 2.6 to 4.0 μm by the applied load of 10 m*N*. The length of the diagonal of the residual impression was from 18 to 28 μm. Thus, changes in microhardness at the small area less than 400 μm^2 were not detected by this experiment. In spite of the same content of EBR, H_V of the injection molded specimen was smaller than that of compression molded one. Earlier report suggested that the interfacial energy increased by the extension of EBR particles decreased the microharness.[12] Small H_V at the injection molded PP surface was explained as low crystallinity of PP by quenching on the mold wall.[20]

We considered that the small H_V was affected not only the interfacial area and the crystallinity but also the shape of distributed particles. So another measurement was carried out at a room temperature (23°C) using a Knoop indenter (H_K), which had anisotropic shape. The long diagonal of a Knoop indenter was set parallel and perpendicular to the flow direction on the cross-cut surface of edge view (Fig. 1). As shown in Figure 9, H_K for "Injection-Perpendicular" was higher than that for "Injection-Parallel". For the compression molded specimen, there was little difference of H_K in parallel and perpendicular directions of the long diagonal. And very important results were shown in Figure 9 that H_K for "Injection-Perpendicular" was close to the H_K for "Compression-Perpendicular and compression-Parallel."

The particle shape through Edge view in Figures 4 and 6 were looked very different. When the direction of the long diagonal coincided to EBR orientation, the microhardness was low. On the other hand, the long diagonal vertical to EBR orientation showed as the same hardness measured with spherically dispersed EBR. Local maximum of H_K at the shear oriented layer was observed for "Injection-Parallel". Therefore, continuity of PP matrix affects mainly to the microdeformation in the PP/EBR blend. In other words, fibrous EBR domain in an injection molded specimen acts as a weak phase in the microhardness. Second, a crystal structure of PP matrix influences the microhardness of the blend.

In addition, FTIR measurement was performed for analyzing EBR content, because uneven distribution of EBR varied the depth profile of the microhardness. Relative absorbance of the ethylene band (720 $cm^{-1)}$ stayed constant to the depth direction (Fig. 10). The variation of the formulation was ignored in this experiment.

Depth profile of shear deformation

The morphology of rubber in the injection molded specimen of PP/EBR is drastically changing from surface to core. It is important for clarifying how the morphology affects the microdeformation in the depth direction. The SAICAS was able to measure continuously shear deformations based on the cutting theory.[21] To compare the anisotropy of the EBR orientation, the shear stress was measured at two

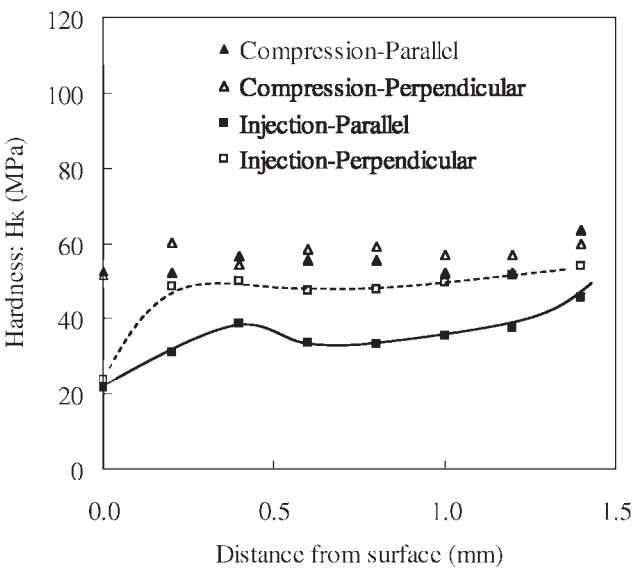

Figure 9 The Microhardness (H_K) profile from surface to core in an injection molded plaque and a compression molded one. The long diagonal of Knoop indenters are applied parallel and perpendicular to the flow direction. Measurement conditions: indentation load 30 m*N*, room temperature.

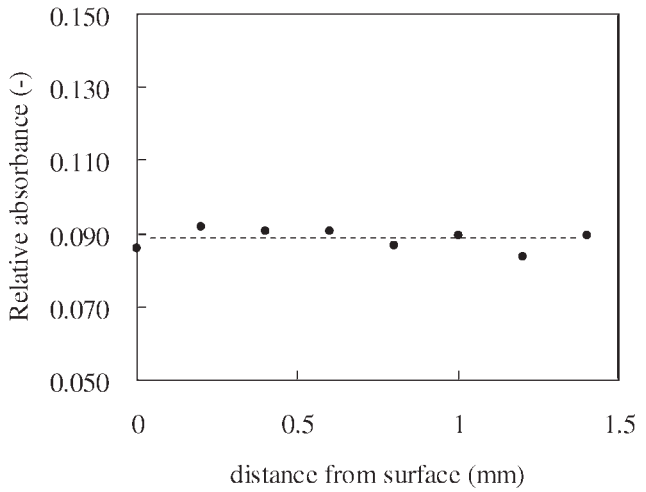

Figure 10 Changes in EBR content along the depth direction measured by micro FTIR with a wave number of 720 cm^{-1}.

cross-cut surfaces, namely FD-ND and TD-ND (Fig. 1). The comparison showed the shear stress on the FD-ND was smaller than that on the TD-ND and the local maximum at the shear oriented layers (Fig. 11). These depth profiles were analogous to that of the microhardness with a Knoop tip (Fig. 9). Thus, fibrous EBR domain in the FD-ND cross section acts as a weak phase in the shear deformation, too. Our aim is the relationship between morphology and the microdeformation neat the surface. As shown in Figure 11, SAICAS cannot measure the shear deformation near the surface. From the cutting theory, at least 20 μm of cutting distance is required for cutting a diamond knife in and out the specimens in the cutting depth 10 μm.

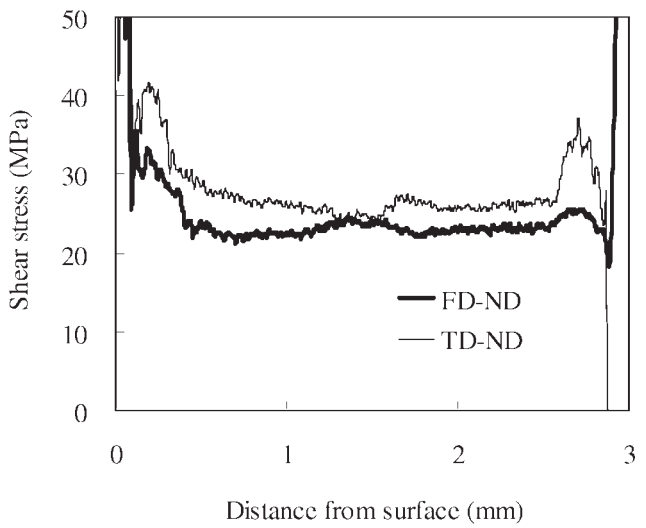

Figure 11 The shear stress profile from surface to core in the injection molded plaque. The cutting tip was applied parallel and perpendicular to the flow direction.

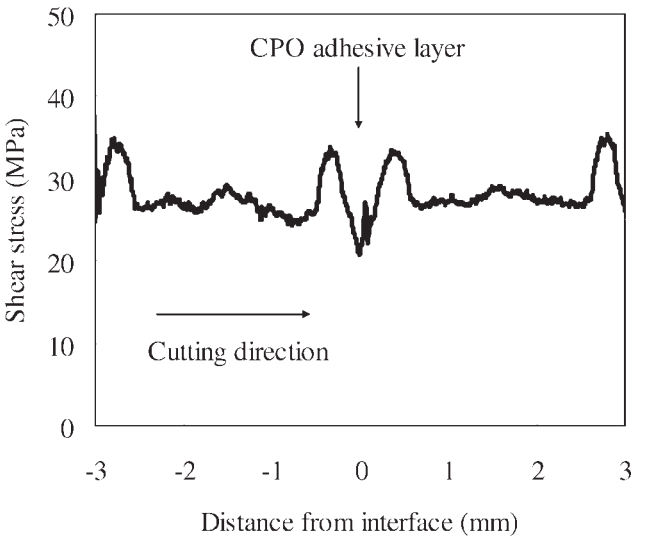

Figure 12 The shear stress profile to depth direction in the injection molded plaques bonded with CPO. The cutting tip was applied perpendicular to the flow direction.

For determining the stress at the surface, two specimens were bonded with CPO (thichness 2.1 μm) and measured by SAICAS [Fig. 2(b)]. Figure 12 is very important, because there are few data which directly measured the continuous profile of mechanical property relating to the injection molding induced hierarchic morphology. The interface indicated the minimum shear stress so that a weak point was predicted to be the surface of the specimen. From our previous work,[22] injection molded PP homopolymer indicated the local maximum of microhardness at the shear oriented layer and minimum at the surface. The behavior of microhardness was mainly caused by crystallinity of PP. We used two methods, microhardness with a Knoop tip and the SAICAS in this study. Morphology of EBR affects mainly anisotropy of the microdeformation. A depth profile of the microdeformation is influenced by crystal structure of matrix PP more strongly than by morphology of EBR.

Application of microhardness and shear stress for peel phenomena

As aforementioned, we showed a weak point of microhardness and shear stress in an injection molded specimen is the surface in the depth direction. In a practical adhesion test on a painted TPO, debonding of paint from TPO substrate occurs at not only the surface but also the inside of the substrate. Figure 13 shows a microphotograph and TEM photograph at the cross-section (FD-ND) of a painted PP/EBR plaque, which was partially peeled by a 180 degrees peel test. Fracture occurred at 0.01 mm depth from surface. The position of fracture is in the

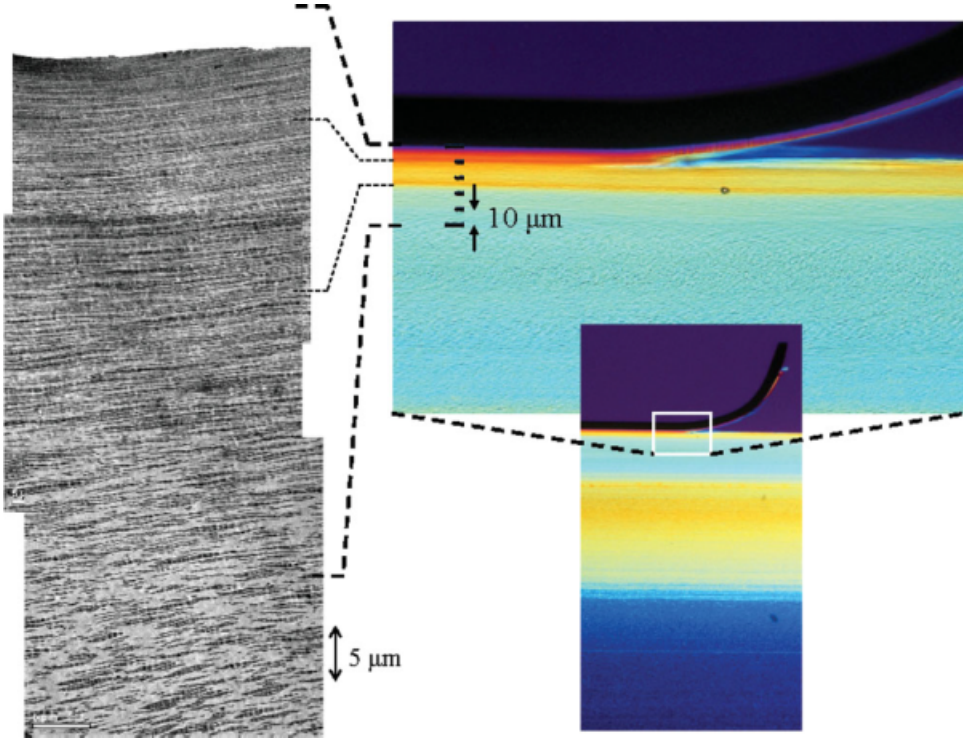

Figure 13 Surface morphology around the fractured position observed by POM and TEM (Edge view). [Color figure can be viewed in the online issue, which is available at www.interscience.wiley.com.]

middle of changing birefringence and EBR orientation.

A possible cause is considered the difference of energy dissipation in the fracture between the peel test and SAICAS. Figure 14 shows schematically directions of a load applied to an injection molded specimen for a peel strength, Knoop hardness and SAICAS. Because the peel direction in Figure 13 is FD, the microdeformation in the specimen is equivalent one on Knoop hardness (TD, ND) and SAICAS (TD-ND). Although the peel mechanism for painted TPO has not been researched extensively before this work, a lot of earlier works for a pressure sensitive adhesive tape has been studied the peel mechanisms, which were based on the Maxwell viscoelastic model or the Griffith theory.[23–25] Adhesive connected between a tape and a substrate is largely stretched and dissipates energy for peeling. As analogy, EBR domain may act like adhesive between the fractured layers. In this study, birefringence caused by PP orientation and EBR orientation are higher near the surface of an injection molded plaque. Injection molded surface has low shear stress compared with the other position in the plaque, but strength at break may high at the deformation of peeling. Although we clarify the depth profile of shear stress at cross-section of an injection molded plaque, the position of cohesive fracture in a peel test needed further study.

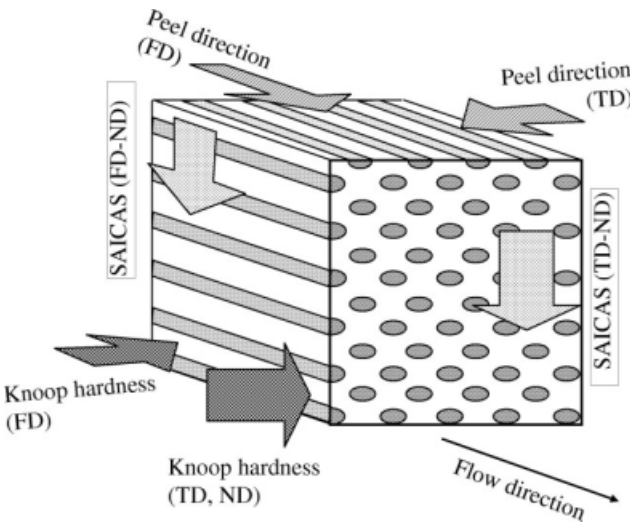

Figure 14 The measurement directions for a peel test, Knoop hardness and SAICAS on an injection molded specimen.

CONCLUSIONS

This study discussed the relationship between microdeformations and morphological distributions of an elastomer phase in a PP/EBR blend at the surface of injection molded specimens.

1. EBR particles were largely deformed from surface to core in the injection molded specimen.

The morphology was quantified by distributions of particle size and circularity. As reference, a compression molded plaque was analyzed. Although the circularity was different in the depth direction of the injection-molded plaque, the area in the depth direction was slightly changed compared with the one in the compression molded specimen. Therefore, breakup and coalescence of EBR particles scarcely occur during the injection process. In addition, morphology at the surface was not quantified because of measuring limit.

2. The deformation of the EBR particles in the depth direction did not coincide to molecular and crystal orientation of PP, which indicated local maximum at the shear oriented layer.
3. From comparison of compression and injection molded specimens, the spherically distributed EBR morphology showed the high microhardness and the particle size was affected little to the hardness. Continuity of the PP matrix was very important for the microdeformation. In other words, the strongly oriented EBR domains acted as a weak layer in the injection molding induced morphology.
4. We succeeded in measuring continuously the depth profile of the shear stress using SAICAS. The profile showed minimum value at the surface and was affected mainly by the crystal structure of PP phase.
5. Injection molded plaques of PP/EBR was painted, and then a 180 degrees peel test was carried out. Debonding position was inner the substrate. The position where cohesive fracture occurred did not coincide to the weak point estimated by SAICAS.

The authors thank S. Ikeuchi and Y. Otsuka for supporting the TEM observation. Finally, Prime Polymer Co., Ltd. is acknowledged for permitting the release of this study.

References

1. Yin, Z.; Yang, J.; Coombs, N.; Winnik, M. A.; Ryntz, R. A.; Yaneff, P. V. Polymer 2007, 48, 1297.
2. Bonnerup, C.; Gatenholm, P. J. Adhes Sci Technol 1993, 7, 247.
3. Tomasetti, E.; Legras, R.; Henri-Mazeaud, B.; Nysten, B. Polymer 2000, 41, 6597.
4. Tang, H.; Martin, D. C. J Mater Sci 2002, 37, 4783.
5. Berta, D. A. In Coatings of Polymers and Plastics; Ryntz, R. A., Yaneff, P. V., Eds. Marcel Dekker: New York, 2003; pp 85–119.
6. Moffitt, M.; Rharbi, Y.; Chen, W.; Tong, J.-D.; Winnik, M. A.; Thurman, D. W.; Oberhauser, J. P.; Kornfield, J. A.; Ryntz, R. A. J Polym Sci B 2002, 40, 2842.
7. Li, J.; Zhang, X.; Qu, C.; Zhang, Q.; Du, R. N.; Fu, Q. J Appl Polym Sci 2007, 105, 2252.
8. D'Orazio, L.; Mancarella, C.; Martuscelli, E.; Cecchin, G.; Corrieri, R. Polymer 1999, 40, 2745.
9. D'Orazio, L.; Cecchin, G. Polymer 2001, 42, 2675.
10. Nitta, K.; Shin, Y.; Hashiguchi, H.; Tanimoto, S.; Terano, M. Polymer 2005, 46, 965.
11. Fakirov, S. J Mater Sci 2007, 42, 1131.
12. Flores, A.; Aurrekoetxea, J.; Gensler, R.; Kausch, H. H.; Baltá Calleja, F. J. Colloid Polym Sci 1998, 276, 786.
13. Michler, G. H.; Baltá-Calleja, F. J.; Puente, I.; Cagiao, M. E.; Knoll, K.; Henning, S.; Adhikari, R. J Appl Polym Sci 2003, 90, 1670.
14. Baltá-Calleja, F. J.; Cagiaoa, M. E.; Adhikarib, R.; Michler, G. H. Polymer 2004, 45, 247.
15. Iwata, A. Techno-Cosmos 2006, 19, 13.
16. Groover, M. P. Fundamentals of Modern Manufacturing; 3rd ed.; Wiley: New York, 2007; pp 486–504.
17. Asbeck, W. K. In Adhesion and Cohesion; Weiss, P., Ed. Elsevier: New York, 1962; pp 101–120.
18. Pötschke, P.; Wallheinke, K.; Janke, A.; Bellmann, C.; Stutz, H.; Heckmann, W. J Macromol Sci B 1999, 38, 527.
19. Viana, J. C. Polymer 2005, 46, 11773.
20. Aurrekoetxea, J.; Sarrionandia, M. A.; Urrutibeascoa, I.; Maspoch, M. L. Polymer 2003, 44, 6959.
21. Nishiyama, I.; Kishima, Y.; Kuroki, T. Zairyou-System 1991, 10, 81.
22. Kobayashi, Y.; Kanno, H.; Hanamoto, Y.; Ando, M.; Kanai, T. J Appl Polym Sci, to appear.
23. Wu, S. Polymer Interface and Adhesion; Marcel Dekker: New York, 1982; 530–554.
24. Mizumachi, H., Ed. Adhesion Science and Technology, OPA Amsterdam: Amsterdam, 1997; pp 703–820.
25. Georgiou, I.; Hadavinia, H.; Ivankovic, A.; Kinloch, A. J.; Tropsa, V.; Williams, J. G. J Adhes 2003, 79, 239.